VYTAUTAS MAGNUS UNIVERSITY
M C M X X I I
ISSN 1392-1134/ eISSN 2345-0371
AGRICULTURAL ENGINEERING
2024, Vol. 56, 1-9 p.
https://doi.org/10.15544/ageng.2024.56.1

LAND COVER MAPPING OF TROPICAL FOREST AREAS USING SPOT IMAGE IN CENTRAL BORNEO

Indarto Indarto, Mahrus Irsyam, Achmad Subagio
Faculty of Agricultural Technology, University of Jember, Indonesia

Abstract

Land cover is fundamental information for understanding human activities' interaction with nature. This information is derived from remotely sensed images. This study analyzes and compares tropical forested areas' land cover (LC) classification results. In this study, we use a SPOT image as the primary input. The study was conducted in Central Borneo and covered 162.60 km2. The image was processed using three algorithms, including NN-MLP, MLC, and ECHO Classifier, with three treatments (2×2, 4×4, and 6×6) sized block of pixels. The classification produces nine (9) land cover classes, i.e., Sparse vegetation area, Dense Vegetation area, Shrubland, Open Water Body, Open Land, Grassland, Mining Area, Pavement Area, and Palm Oil Area. The three algorithms can produce land cover maps with kappa and an overall accuracy value of more than 85%. However, NN-MLP has better accuracy than other algorithms (MLC and ECHO), with a kappa value of 90.72% and an overall accuracy of 93.88%.

Keywords: *SPOT, Land cover, Classification, Forested area, Central Borneo.*

Received 2024-08-11, accepted 2024-10-21

1. Introduction

The land cover map that brings land-use status is applied to urban and regional planning, conservation and management of natural resources, and socioeconomic and environmental management [1], [2]. Remote sensing is a technique to produce land cover maps. SPOT 6 is one of the high-resolution satellites commonly used to create land cover maps. However, this image has a pixel size smaller than the actual object size, with high heterogeneity [3].

Multispectral classification methods commonly used based on the data distribution can use a parametric approach, such as a maximum likelihood, or a non-parametric approach, such as an artificial neural network [4]. In many remote sensing applications, pixel-based classification, such as Maximum Likelihood Classifier (MLC) and Extraction and Classification of Homogeneous Objects (ECHO), has been used widely [5]–[7]. The ECHO algorithm is a spatial pre-processing method developed by [8]. ECHO divides the image into cells consisting of pixels with a spectrally homogeneous spectrum into small groups. If there is a statistical similarity, individual cells are compared to neighboring fields and annexed. Finally, the homogeneous objects are classified using maximum likelihood criteria [9], [10].

Recently, [11] presented Neural Network-Multi Layer Perceptron (NN-MLP) in pixel classification to solve the XOR problem. This algorithm is one of the artificial neural networks that provides a supervised classification method for multi-band passive optical remote sensing data. The NN-MLP algorithm assumes that the various classes are no longer linearly separable and cannot be resolved using a minimum distance or maximum likelihood classifier. The NN-MLP classifier creates an artificial neural network consisting of many layers of nodes: the input layer, hidden layer, and output layer. Classification problems can be solved by dividing the cluster in the input space into several sub-clusters before classification and then combining them again after classification [12].

The objectives of this study are to (1) Produce land cover maps in a tropical forested area using three classification algorithms and (2) Compare the classification result obtained using high-resolution imagery.

2. Materials and Methods

2.1 Study Site and Input Data

This research area is characterized by forest, with most of the land covered in dense vegetation, located in Central Borneo, and comprises an area of 162.60 km2 (Figure 1). This study is part of the development plan for the Food Estate Area organized by the Ministry of Defense of the Republic of Indonesia to strengthen national food security (Business Plan).

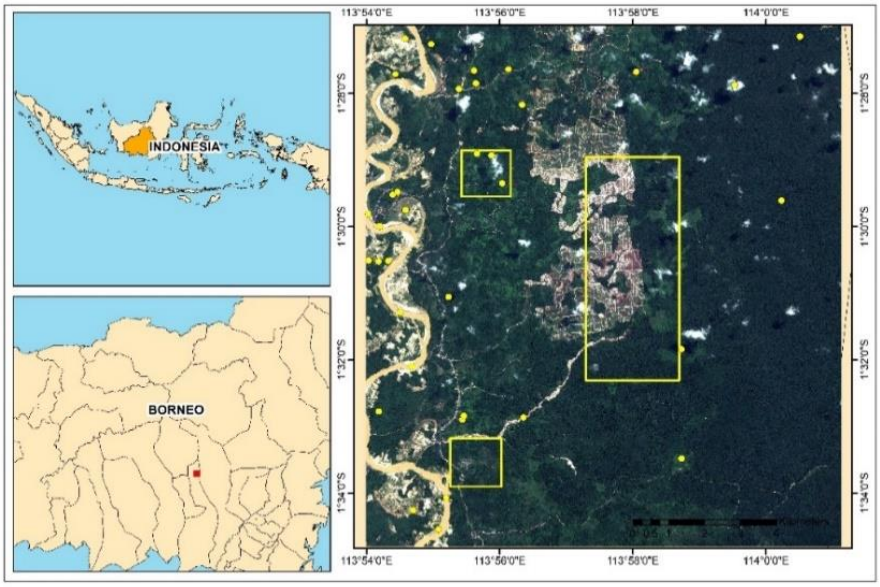

Fig. 1. SPOT images of Study site

The project supplied the data for planning and designing the site plan, site grading, cutting and land clearing. Figure 1 presents the SPOT images, selected sites for training areas (yellow point), and three subset areas (yellow rectangle). The field survey was conducted to reference creating a training area. Field data is collected using GPS as a survey point and a digital camera to determine the current field condition and adjust with the class to be classified.

SPOT images with the minimum cloud cover were used as a primary input to produce the LULC maps. Table 1 shows the metadata of the raw SPOT image. SPOT comprises two twin satellites, i.e., SPOT 6 and 7, providing resource and human activity analysis, forecasting, monitoring, and management data. They are in the same orbit as a true constellation and are phased 180° apart [13].

Table 1. SPOT Image metadata

Date Acquired	Cloud Cover	Data Type/Collection Category	Sun Elevation (°)	Sun Azimuth (°)
7/15/2019	3.57	SPOT 6 PMS ORT	50.6875021203	50.8537619986

The area (percentages and number samples in pixels) of each training area are shown in Table 2. The training area is a small image containing the predictor variables measured in each sampling unit. Training areas represent a cover type with the geography information of a region and spectral properties of the cover class [14 –16].

Table 2. Summary of the training areas

Class	Number of samples (pixels)	Percentage (%)	Area (km2)
Sparse vegetation (SV)	3097	38.25	0.12
Dense Vegetation (DV)	2400	29.59	0.09
Sandy Road (SR)	304	3.74	0.01

Table 2. Summary of the training areas (continuation)

Open Water Body (OWD)	1277	15.74	0.05
Open land (OL)	610	7.62	0.02
Grass Land (GL)	266	3.25	0.01
Minning Area (MA)	134	1.67	0.01
Pavement area (PA)	12	0.14	0
Palm oil area (POA)	0	0	0
Total	8100	100	0.31

Following the Indonesian national standard 7645:2014 [17], nine (9) classes of Land Cover were created. In addition, a field survey was conducted from September until October 2020 to determine and capture the current field condition. Figure 2 shows the photos of the training area clipped and selected from the RGB image of SPOT and ground photos captured using a digital camera.

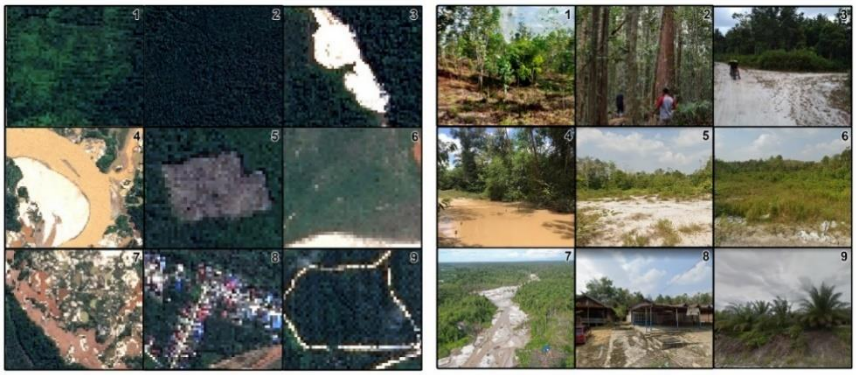

Fig. 2. RGB images and ground photos of training areas

Furthermore, nine (9) classes are identified as follows:

1. Sparsely Vegetated area (SV) represents all surface features on the ground, including a mixture of annual trees and seasonal crops.
2. Annual vegetation types, such as primary tropical and secondary forests or mixed plantations, dominate the dense Vegetation area (DV).
3. Sandy Road (SR) is a road network with sand cover. This road usually connects the village and the oil palm plantation block.
4. Open water body (OWB) visualized surface features such as rivers, ponds, and water bodies.
5. Open Land (OL) represents an open area not developed for built-up areas and is covered with little vegetation.
6. Grassland (GL) is an area covered by wildlife grass cleared by dense trees.
7. The mining area (MA) represents the mining area. This region's small gold mining areas spread almost all over the river.
8. Pavement area (PA) represents an area that has undergone development in settlements or other public facilities.
9. Palm Oil Areas (POA) visualized the palm oil plantation areas.

2.2 Data Processing

The data processing procedure consists of pre-processing, classification process, and post-processing. Data processing and analysis were performed using QGIS 3.14.

A. Pre-Processing

Pre-processing consists of atmospheric correction, band composite, image mosaic, and clipping. A Semi-Automatic Classification Plugin (SCP) was used for the pre-treatment process. The plugin is available in QGIS 3.14. Atmospheric correction removes the atmospheric effect that scatters the signal before being recorded by a remote sensing sensor [18].

B. Classification Algorithm

Image classification was performed using three algorithms, specifically Extraction and Classification of Homogeneous Object (ECHO), Gaussian Maximum Likelihood (GML), and Neural Network-Multi Layer Perceptron (NN-MLP). ECHO variety was used in this study, consisting of 2x2, 4x4, and 6x6-sized blocks of pixels. Moreover, NN-MLP was performed using QGIS software.

C. Post Processing

The classification result is accomplished post-treatment using a Majority filter and Boundary-clean. Furthermore, an accuracy test is carried out to determine classification accuracy results. An accuracy assessment was performed using a confusion matrix, and the total percentage of the area after post-treatment was calculated. The final results are five thematic maps of LULC. In addition, three subsets were created to show each algorithm's difference in more detail.

3. Result and Discussion

3.1 Accuracy Assessment

The classification process produces nine (9) land cover classes, i.e., SV, DV, SR, OWB, OL, GL, MA, PA, and POA. In general, all treatments produce good classification accuracies. Table 3 shows the producer's, user's, overall, and Kappa accuracy values of each land cover class from five algorithms. This study produced the highest kappa and overall accuracy using the NN-MLP algorithm (Kappa: 90.72%, Overall: 93.88%). Neural network algorithms are superior in handling complex phenomena (heterogeneous) compared to other algorithms [19]. In comparison, the lowest kappa and overall accuracy were produced by MLC (Kappa: 87.40%, Overall: 92.01%).

Table 3. Each class's accuracy (reliability, reference, kappa, and overall)

Class	NN-MLP		MLC		ECHO 2X2		ECHO 4X4		ECHO 6X6	
	Rel. acc	Ref. acc	Rel. acc	Ref. acc	Rel. acc	Ref. acc	Rel. acc	Ref. acc	Rel. acc	Ref. acc
SV	82.19	83.33	81.25	90.51	81.28	83.52	80.43	84.09	89.66	100
DV	83.28	95.65	81.14	90.48	85.48	93.31	85.90	94.58	95.17	90.46
SR	96.56	98.10	95.99	96.67	97.02	96.17	96.89	96.48	96.39	95.51
OWB	92.19	92.67	87.32	84.26	92.31	87.05	91.93	88.07	85.71	86.57
OL	89.15	92	100	90.76	100	96.30	100	96.15	77.88	100
GL	92.78	83.33	85.28	85.28	83.27	90.87	83.63	88.73	80.16	80.16
MA	100	90	83.08	87.80	86.99	90.68	91.30	84.00	85.71	98.18
PA	86.89	80.30	80.17	82.20	80	88.68	81.55	89.20	82.28	85.15
POA	100	82.16	100	82.83	84.78	85.25	83.50	81.07	96.05	82.52
Kappa	90.72		87.40		88.76		88.78		87.56	
Overall	93.88		92.01		93.00		93.03		92.28	

Key: Rel. Acc = Reliability Accuracy, Ref. Acc = reference accuracy.

Furthermore, individual accuracies of each algorithm produce relatively good value (>80%). However, there is ambiguity in distinguishing SV, DV, and GL classes. Individual accuracy consists of two types, namely Reference accuracy and Reliability accuracy. Reference accuracy is a measure of omission error. This accuracy measures how the actual land cover types can be appropriately classified. Reliability accuracy measures errors of omission, representing the possible classified pixel values that match the actual land cover type [4], [20 – 22].

3.2 Classified Maps

Figure 3 shows the classified maps produced by the five (5) treatments using three algorithms: A: NN-MLP, B: MLC, C: ECHO 2x2, D: ECHO 4x4, and E: ECHO 6x6. The black colour is unclassified (cloud and cloud shadow).

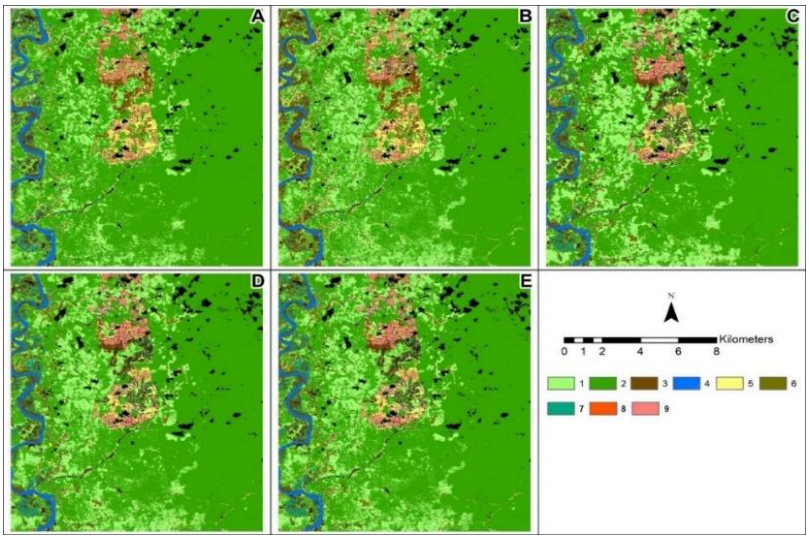

Fig. 3. Overall result

Table 4. Classified area extends in (ha) and percentage (%) of the total area

Class	NN-MLP		MLC		ECHO 2X2		ECHO 4X4		ECHO 6X6	
	Area (ha)	%	Area (ha)	%	Area (ha)	%	Area (ha)	%	Area (ha)	%
SV	2033	13.43	2866	19.12	2622	17.58	2674	17.96	2615	17.57
DV	10512	69.46	9395	62.68	9414	63.10	9363	62.89	9417	63.26
SR	735	4.86	923	6.16	697	4.67	660	4.43	656	4.41
OWB	325	2.15	235	1.57	225	1.51	230	1.54	231	1.55
OL	542	3.58	612	4.08	414	2.78	414	2.78	414	2.78
GL	485	3.20	617	4.12	759	5.09	745	5	748	5.02
MA	245	1.62	109	0.73	469	3.14	487	3.27	490	3.29
PA	0	0	9	0.06	23	0.15	23	0.15	23	0.15
POA	257	1.70	223	1.49	295	1.98	292	1.96	293	1.97
Total	15134	100	14989	100	14918	100	14888	100	14887	100

The ECHO algorithms combined by 2x2, 4x4, and 6x6 pixel groups have done relatively similar areas of each class. The NN-MLP algorithm generally produces classification results closest to the field condition. For example, dense vegetation covers about 69.46% of the study area based on the NN-MLP algorithm classification. However, ECHO can classify the PA class as covering 0.15% of the study area.

Misclassification may occur because the ROI for the training area is too significant, making the land cover sample not 100% homogeneous. As a result, a mixed pixel value does not represent the object's appearance in the field. In addition, the SPOT image used only consists of three bands (RGB), so it is less clear to distinguish vegetation and non-vegetation when compared to images with a composition of 4 bands (RGB and NIR).

3.3 Land Cover in Subset 1

This Subset (Figure 4) shows that NN-MLP and MLC are not better at classifying the Pavement Area (PA) class when compared to ECHO. However, the PA class is ambiguous because the field condition shows that the roof of the settlement is the same colour as the vegetation and shrubs. In addition, many use iron as the roof, which is visualized as white in the image and not correctly classified and considered a cloud (unclassified) due to the sunlight reflection effect. ECHO algorithm with three treatments, i.e., 2x2, 4x4, and 6x6 group pixels, produces a PA class of 2 ha (1.33%), while it could not be classified in other algorithms.

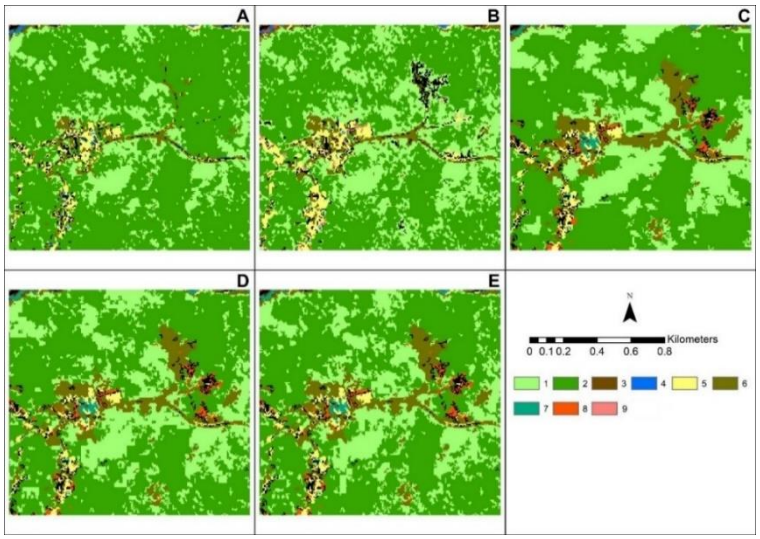

Fig. 4. Subset 1

Table 5. Percentage area of subset 1

Class	NN-MLP		MLC		ECHO 2X2		ECHO 4X4		ECHO 6X6	
	Area (ha)	%	Area (ha)	%	Area (ha)	%	Area (ha)	%	Area (ha)	%
SV	30	20	46	30.46	40	26.67	41	27.33	40	26.67
DV	110	73.33	89	58.94	88	58.67	87	58	88	58.67
SR	0	0	1	0.66	0	0	0	0	0	0
OWB	0	0	0	0	-	0	0	0	0	0
OL	4	2.67	7	4.64	4	2.67	4	2.67	4	2.67
GL	6	4	7	4.64	15	10	15	10	15	10
MA	-	0	-	0	1	0.67	1	0.67	1	0.67
PA	0	0	0	0	2	1.33	2	1.33	2	1.33
POA	0	0	1	0.66	-	0	-	0	-	0
Total	150	100	150	100	150	100	150	100	150	100

3.4 Land Cover in Subset 2

Subset 2 is ROI covers about 1.31 km^2. This subset was dominated by dense vegetation, sparse vegetation, and shrubs. The black colour in the map (Figure 5) is cloud cover and shadow.

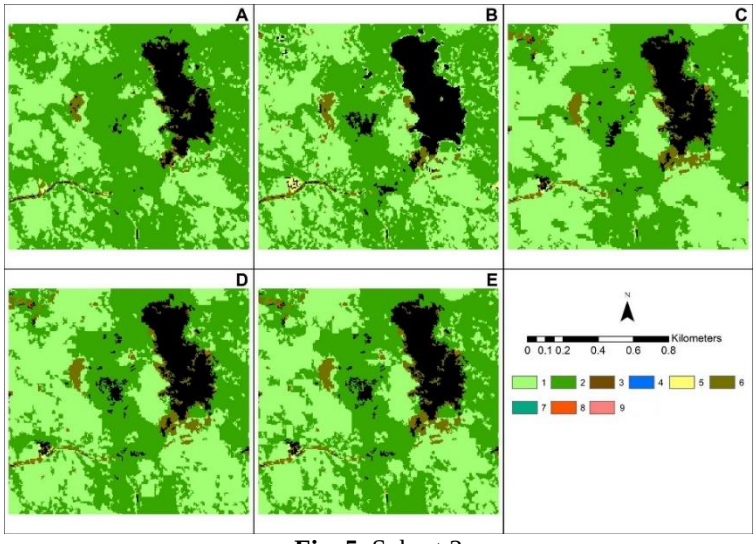

Fig. 5. Subset 2

Table 6 presents the percentage area of each class in subset 2. ECHO shows better results than the two algorithms (NN-MLP and MLC) in calculating grassland (GL), which has the result of 4.69% of the total study area. Then, NN-MLP shows an excellent ability to calculate dense vegetation of 60.31% of ROI. In conclusion, the NN-MLP can calculate the dense vegetation area better than other algorithms (MLC and ECHO).

***Table* 6**. Percentage area of subset 2

Class	NN-MLP		MLC		ECHO 2X2		ECHO 4X4		ECHO 6X6	
	Area (ha)	%	Area (ha)	%	Area (ha)	%	Area (ha)	%	Area (ha)	%
SV	48	36.64	58	46.03	60	46.88	62	48.82	59	46.09
DV	79	60.31	64	50.79	62	48.44	59	46.46	63	49.22
SR	-	0	-	0	-	0	-	0	-	0
OWB	0	0	-	0	-	0	-	0	-	0
OL	0	0	0	0	0	0	0	0	0	0
GL	4	3.05	4	3.17	6	4.69	6	4.72	6	4.69
MA	-	0	-	0	0	0	0	0	0	0
PA	0	0	-	0	0	0	0	0	0	0
POA	-	0	0	0	-	0	-	0	-	0
Total	131	100	126	100	128	100	127	100	128	100

3.5 Land Cover in Subset 3

In Subset 3 (Figure 6) and table 7, land cover is dominated by vegetation (SV and DV), sandy road (SR), and palm oil area (POA).

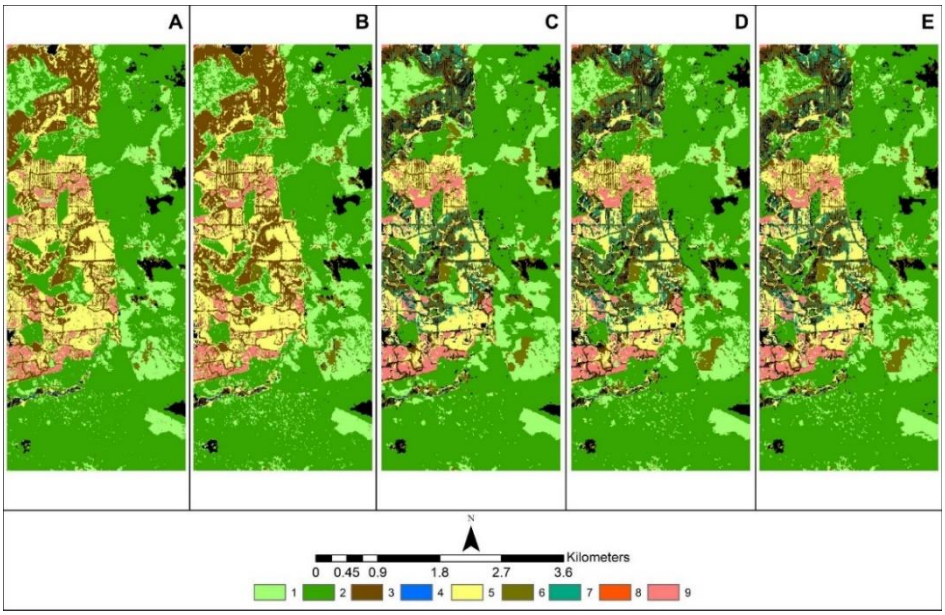

Fig. 6. Subset 3

There are different classification results among NN-MLP, MLC, and ECHO. The ECHO algorithm is close to where the mining area (MA) could be classified appropriately. A mining area (MA) could be found along the river that passes through the palm plantation area (POA), while other algorithms could not classify it. It is probably caused by the composition of the mining area (MA) mixture with the sandy road (SR), which has the same colour in the image visualization.

Table 7. Percentage area of subset 3

Class	NN-MLP		MLC		ECHO 2x2		ECHO 4x4		ECHO 6x6	
	Area (ha)	%	Area (ha)	%	Area (ha)	%	Area (ha)	%	Area (ha)	%
SV	158	12.38	195	15.40	175	14.36	176	14.53	175	14.42
DV	689	54.00	620	48.97	625	51.27	618	51.03	621	51.15
SR	168	13.17	193	15.24	121	9.93	119	9.83	119	9.80
OWB	1	0.08	1	0.08	-	0	-	0	-	0
OL	187	14.66	176	13.90	139	11.40	139	11.48	139	11.45
GL	30	2.35	39	3.08	57	4.68	57	4.71	59	4.86
MA	1	0.08	0	0	54	4.43	54	4.46	54	4.45
PA	-	0	1	0.08	1	0.08	1	0.08	1	0.08
POA	42	3.29	41	3.24	47	3.86	47	3.88	46	3.79
Total	1276	100	1266	100	1219	100	1211	100	1214	100

4. Conclusion

LULC was conducted using a SPOT 6 image with three algorithms and five treatments (NN-MLP, MLC, and ECHO 2x2, 4x4, and 6x6). The classification produces five thematic maps with nine (9) classes, i.e., Sparse Vegetation (SV), Dense Vegetation (DV), Sandy Road (SR), Open Water Body (OWB), Open Land (OL), Grass Land (GL), Mining Area (MA), Pavement Area (PA), and Palm Oil Area (POA). In more detail, three subsets were used to determine each algorithm's differences. The three algorithms can produce land cover maps with kappa and an overall accuracy value of more than 85%. However, NN-MLP has better accuracy than other algorithms (MLC and ECHO), with a kappa value of 90.72% and an overall accuracy of 93.88%. The other two classes (i.e., heterogeneous agricultural land and sparse vegetation area) are separated by ambiguity.

.

Acknowledgements

This publication is a reworking of an undergraduate project ("Skripsi") as part of the project "Mapping and planning for cassava food estate in Gunungmas Regency, Central Kalimantan, in the year 2022, coordinated by Indarto.

References

[1] M. Li, S. Zang, B. Zhang, S. Li, and C. Wu, "A review of remote sensing image classification techniques: The role of Spatio-contextual information," *Eur. J. Remote Sens.*, 2014, doi: 10.5721/EuJRS20144723.

[2] Y. Tu *et al.*, "Improved Mapping Results of 10 m Resolution Land Cover Classification in Guangdong, China Using Multisource Remote Sensing Data With Google Earth Engine," *IEEE J. Sel. Top. Appl. Earth Obs. Remote Sens.*, vol. 13, pp. 5384–5397, 2020, doi: 10.1109/JSTARS.2020.3022210.

[3] I. L. Sari and S. Fildes, "Land cover classification using Object-Based Image Analysis of SPOT-6 imagery for land cover and forest monitoring in Nagan Raya, Aceh - Indonesia," *Int. J. Adv. Sci. Eng. Inf. Technol.*, 2017, doi: 10.18517/ijaseit.7.6.3426.

[4] J. R. Jensen, "Introductory Digital Image Processing (3rd edition). Prentice Hall.," *Int. J. Remote Sens.*, 2005.

[5] M. H. Al-Jiboori, M. J. Abu-Alshaeer, and M. M. Ahmed, "Impact of land surface changes on air temperatures in Baghdad," Oct. 2020. [Online]. Available: http://earthexplorer.usgs.gov/

[6] A. K. Basukala, C. Oldenburg, J. Schellberg, M. Sultanov, and O. Dubovyk, "Towards improved land use mapping of irrigated croplands: performance assessment of different image classification algorithms and approaches," *Eur. J. Remote Sens.*, vol. 50, no. 1, pp. 187–201, Jan. 2017, doi: 10.1080/22797254.2017.1308235.

[7] J. Hogland, N. Billor, and N. Anderson, "Comparison of standard maximum likelihood classification and polytomous logistic regression used in remote sensing," *Eur. J. Remote Sens.*,

2013, doi: 10.5721/EuJRS20134637.
[8] R. L. Kettig and D. A. Landgrebe, "Classification of Multispectral Image Data by Extraction and Classification of Homogeneous Objects," *IEEE Trans. Geosci. Electron.*, 1976, doi: 10.1109/TGE.1976.294460.
[9] D. Lu *et al.*, "Land use/cover classification in the brazilian amazon using satellite images," *Pesqui. Agropecu. Bras.*, vol. 47, no. 9, pp. 1185–1208, 2012, doi: 10.1590/S0100-204X2012000900004.
[10] C. A. Berlanga-Robles and A. Ruiz-Luna, "Land use mapping and change detection in the coastal zone of northwest Mexico using remote sensing techniques," *J. Coast. Res.*, 2002.
[11] A. Crabbe, T. Cahy, B. Somers, L. P. Verbeke, and F. Van Coillie, "Neural Network MLP Classifier," 2020.
[12] N. Kushwaha, N. K. Mendola, S. Ghosh, A. D. Kachhvah, and S. Jalan, "Machine Learning Assisted Chimera and Solitary States in Networks," *Front. Phys.*, 2021, doi: 10.3389/fphy.2021.513969.
[13] Astrium, *SPOT 6 & SPOT 7 Imagery User Guide*. 2013.
[14] L. Černá and M. Chytrý, "Supervised classification of plant communities with artificial neural networks," *J. Veg. Sci.*, vol. 16, no. 4, pp. 407–414, Aug. 2005, doi: https://doi.org/10.1111/j.1654-1103.2005.tb02380.x.
[15] A. K. Skidmore, "Unsupervised training area selection in forests using a nonparametric distance measure and spatial information," *Int. J. Remote Sens.*, vol. 10, no. 1, pp. 133–146, Jan. 1989, doi: 10.1080/01431168908903852.
[16] J. Al-doski, S. B. Mansor, and H. Z. M. Shafri, "Image Classification in Remote Sensing," *J. Environ. Earth Sci.*, vol. 3, no. 10, pp. 141–147, 2013.
[17] BSN, "Standar Nasional Indonesia (SNI) 7645:2014 tentang Klasifikasi Penutup Lahan," p. 28, 2014.
[18] N. Hoepffner and G. Zibordi, "Optical remote sensing of coastal waters," in *Encyclopedia of Ocean Sciences*, 2019. doi: 10.1016/B978-0-12-409548-9.10812-7.
[19] M. S. Rini, "Kajian kemampuan metode neural network untuk klasifikasi penutup lahan dengan menggunakan Citra Landsat-8 OLI (kasus di Kota Yogyakarta dan sekitarnya)," *Geomedia Maj. Ilm. dan Inf. Kegeografian*, vol. 16, no. 1, Aug. 2018, doi: 10.21831/gm.v16i1.20974.
[20] S. S. Rwanga and J. M. Ndambuki, "Accuracy Assessment of Land Use/Land Cover Classification Using Remote Sensing and GIS," *Int. J. Geosci.*, 2017, doi: 10.4236/ijg.2017.84033.
[21] R. G. Congalton, "A review of assessing the accuracy of classifications of remotely sensed data," *Remote Sens. Environ.*, vol. 37, no. 1, pp. 35–46, 1991, doi: 10.1016/0034-4257(91)90048-B.
[22] J. B. Campbell, *Introduction to Remote Sensing*, 4th ed. New York: The Guilford Press, 2008.

Author for contacts
Indarto Indarto
University of Jember,
Department Agricultural Engineering,
Jl. Kalimantan 37, Kampus Tegalboto, Sumbersari, Jember, 68121, East Java, Indonesia,
e-mail: indarto.ftp@unej.ac.id
https://orcid.org/0000-0001-6319-6731
Scopus Author ID : 57194602119
Loop profile : 457083
Researcher ID : AAI-1555-2020